行政院國家科學委員會專題研究計畫成果報告

LPCVD 製程設備中加熱系統之熱輻射量測及晶圓熱應力分析(III)

計畫編號：NSC 88-2218-E-009-003
執行期限：87 年 8 月 1 日至 88 年 7 月 31 日

整合型計畫主持人：
總計畫主持人：林清發　國立交通大學機械系教授
子計畫主持人：曲新生　國立交通大學機械系教授

中文摘要

本研究應用傅氏轉換紅外線頻譜儀來量測快速熱程序爐中不同加熱燈源的放射頻譜。本研究所使用之傅氏轉換紅外線頻譜儀係 Bomem 公司出品，型號為 MB-154；所使用之加熱燈源係 Osram 公司出品，型號分別為 No. 64573 和 No. 64743 的石英鎢絲鹵素燈泡。量測其在不同的電壓下之放射頻譜，以了解這個燈泡於波長 0.7–20 μm 範圍放出輻射熱能的情形。從量測到的結果顯示，鹵素燈泡的放射頻譜是由相當於鎢絲(1–4.5 μm)、受熱石英管(4–9 μm)及燈源基座(9–20 μm)之輻射源的三個放射曲線所組成。增高燈泡的電壓將使鎢絲的溫度升高。原則上，仍是遵守蒲郎克黑體輻射及威恩定律。這些相當於 2000–2600K 鎢絲溫度之加熱燈源的放射頻譜的峰值大約在 1.9–2.5 μm 的波長範圍或 4000–5200 cm^{-1} 的波數範圍。

關鍵字：快速熱程序，加熱燈源，放射頻譜，傅氏轉換紅外線頻譜儀

Abstract

The emission spectrum measurement of the rapid thermal processing (RTP) heating source by Fourier Transform Infrared (FTIR) spectroscopy is presented. The work has been carried out on two quartz-tungsten-halogen lamps of OSRAM type No. 64573 and No. 64743 at the different lamp voltages by Bomem MB-154 FTIR spectrometer from 0.7 μm to 20 μm. From our present experimental measurement results, it is found that the emission spectrum is superposed by three spectral curves located in the range of about 1–4.5 μm, 4–9 μm and 9–20 μm, respectively, corresponding to the emission from the tungsten filament, the warm quartz glass tube and the base. Increasing the voltage of the lamp will increase the tungsten filament temperature. It also shows that the results are principally in good agreement with the Planck's distribution law and Wien's displacement law. The spectral peak output of these heating sources, corresponding tungsten filament temperatures from about 2000K to 2600K, range from 1.9–2.5 μm (4000–5200 cm^{-1}).

Keywords: rapid thermal processing (RTP) heating source, emission spectrum, Fourier Transform Infrared (FTIR) spectroscopy

1. Introduction

Rapid thermal processing (RTP) with an incoherent heating source is used to fabricate microelectronic devices through various processes. In RTP a wafer is quickly processed by the heating source with visible and/or infrared radiation from a lamp array. If the spectral absorptive properties of the wafer to be heated are consistent with the emission spectrum of the heating source, the rapid thermal processing will be in good performance efficiency.

The initial driving force for the development of RTP technique was primarily due to the fact that at elevated temperatures the short time processing feature results in the suppression or reduction of a number of undesirable thermally driven physical and chemical effects (Singh, 1988). The photoeffects from the heating sources play a significant role in diffusion mechanisms and in improving the quality of the processed wafer (Noel et al, 1998; Singh et al, 1991). Timans (1996) also pointed out that the radiation in RTP is complicated and heavily depends on the radiative properties of materials—the heating source and the processed wafer. The different spectral contents of the heating source can result in different physical and chemical phenomena on the illuminated wafer in RTP.

Temperature uniformity across the wafer during all processing continues to be a main obstacle for full acceptance of RTP into manufacturing. A change in spectral distribution of the radiative properties (the wafer or the heating source) is a source of temperature non-uniformity for RTP systems (Wong, 1995). Furthermore, optical pyrometers are probably the most widely used temperature sensor for RTP systems (Roozeboom and Parekh, 1990; Sorrell et al, 1994). However, it is easily interfered by the heating sources. We should minimize the optical noise reaching the pyrometer aperture and maximize the true wafer temperature signal. To be able to proceed with the simulations of RTP, a thorough understanding of the radiant emission spectrum of the heating source is essential for the development of RTP systems.

Fourier transform infrared (FTIR) spectroscopy is a major analytical technique that has widely been used by chemists (Griffiths and Haseth, 1986). FTIR has brought additional merits such as high sensitivity, high precision, quickness of measurement, and extensive data processing capability. Sikka (1991) employed an FTIR spectrometer, allowing him to measure high temperature normal spectral emittance of silicon carbide based materials ranging from 1 μm to 9 μm in a single run. Zhou et al. (1995) reported the epi-film thickness measurement using emission FTIR spectroscopy. They had successfully measured epitaxial silicon film thickness on heavily doped silicon substrates by using the heated wafer as the infrared source. Recently, Ravindra et al. (1998) studied the temperature-dependent emissivity of silicon-related materials and structures in RTP using a spectra emissometer, which consisted of a FTIR spectrometer designed specially to facilitate simultaneous measurements of surface spectral emittance and temperature.

In this study, the FTIR measurement of the emission spectrum of the heating source for RTP system is presented. The work has been carried out on two quartz-tungsten-halogen lamps of OSRAM at different lamp voltages using Bomem Michelson series MB-154 FTIR spectrometer ranging from 0.7 μm to 20 μm.

2. Experimental Investigation

In commercial RTP systems three heating source types are commonly used: the tungsten-halogen lamp, the long-arc noble gas discharge lamp, and the continuous resistively heated bell jar.

The mainstay in RTP heating sources is the tungsten-halogen lamp (Roozeboom, 1993). The main advantages of the tungsten-halogen lamp are its high life/price and power/filament length ratios, and its compact power unit. The OSRAM tungsten-halogen low voltage (120V, 1000W) lamp type No. 64573 and No. 64743 were selected as the RTP heating source in our present experimental measurements.

Description of the experimental apparatus

A Bomem Michelson series MB-154 FTIR spectrometer equipped with a deuterated triglycine sulfate (DTGS) detector (0.8–40 μm) and a wide-band (0.7–20 μm) ZnSe substrate beam splitter was used to collect the emission. Fig. 1 shows the general arrangement of the instrument used in the present study. The spectrometer is a self-contained unit consisting of one sample compartment and a sealed interferometer compartment. The sample compartment is enclosed in a purge cover provided with an access door. The whole system contains a stabilized internal light source, a Michelson interferometer, an infrared-transmitting beam splitter, a Helium-Neon laser for measurement of the scan position, power supplies and electronic assemblies. They are interfaced with a computer for data acquisition of the measured emission. The cast aluminum compartment is sealed to prevent the entry of dust and moist air, which could erode the beam splitter. It is noted that Bomem MB-154 spectrometer is a single substrate self-compensating beam splitter and a permanent alignment interferometer. Besides of the internal light source, there is an optional emission port for the external light source on Bomem MB-154 FTIR system. Instead of spatially separating the optical frequencies, the FTIR spectrometer modulates all wavelengths simultaneously with distinct modulation frequencies for each wavelength.

Experimental procedure

When starting at room temperature, the spectrometer would need about an hour to allow its temperature to stabilize. Water vapor and carbon dioxide could be purged from the optical path of spectrometer by a flow of dry nitrogen. The purge flow should be switched on at least 15 minutes prior to the start of spectroscopic work, at a flow rate of 15 liters/minute for the sample compartment, and 2.5 liters/minute for the interferometer compartment. When measuring emission spectroscopy for the lamps by the emission port on Bomem MB-154 FTIR system, the internal light source must be switched off and there was no wafer in the sample compartment. An instrument calibration step is required. The emission spectrum of a temperature-calibrated blackbody should firstly be recorded. Then, by comparing the recorded emission spectrum of the blackbody to the theoretical emission spectrum of a blackbody at the same temperature, the instrument response function can thus be evaluated.

For the high filament temperature of RTP heating source, we selected a MIKRON M330 Blackbody Calibration Source (800–3000°C) as our temperature-calibrated blackbody. Its temperature was checked by both Infrared thermometer OS3709 and K-type thermocouple from 900°C to 1100°C at every 50°C. During the experimental measurements, the blackbody was placed close to the FTIR spectrometer so that the blackbody was next to the window of the emission port on the FTIR spectrometer. Thus, the emission from the blackbody could arrive at the interferometer after a short travel and could be collected over a large solid angle to maximize the signal-to-noise ratio. The distance between the emission port and the blackbody is about 5 cm, and there is no optics between them. The emission spectra of our temperature-calibrated blackbody at 1100K, 1200K and 1300K were collected with a 4 cm^{-1} resolution and by spectral averaging of 20 scans ranging from 0.7–20 μm. Subsequently, the emission spectra from the lamps at 30, 50 and 70 Volt were also collected on the same experimental condition. It took about 1 min to acquire one sample spectrum with the Bomem MB-154 FTIR spectrometer. Simultaneously, the lamp temperatures were measured with Infrared thermometer OS3709. Once the measurements was completed, the lamp was switched off and the emission was immediately measured again with a 4 cm^{-1} resolution but spectral averaging of only one scan to investigate the background or the other radiation.

3. RESULTS AND DISCUSSION

Table 1 shows the results of checking the blackbody temperature (MIKRON M330 Blackbody Calibration Source) from 900°C to 1100°C by both Infrared thermometer OS3709 and K-type thermocouple at every 50°C. The differences, between M330 Blackbody setting temperature and temperature measured by Infrared thermometer OS3709 and K-type thermocouple, range from 0.4–5.5°C and 5–7°C, respectively. The greatest difference between setting temperature and measured temperature is less than 0.75%.

Since the wavelength is frequently employed for surface emission and absorption, the emission spectrum figures in present paper are plotted in wavelength scale. Figs. 2(a) and 2(b) show the measured emission spectra of the temperature-calibrated blackbody at 1100K, 1200K and 1300K for the instrument enclosure without and with nitrogen gas purge, respectively, during experiment. It can be seen, comparing Fig. 2(a) with Fig. 2(b), that the response (emissive power) without nitrogen gas purge at the absorption bands of water vapor (H_2O, around 1.38, 1.87, 2.7 and 6.3 μm) and carbon dioxide (CO_2, around 2.0, 2.7, 4.3 and 15 μm) are reduced. The measurement results are in good agreement with the experimental works of Edwards (1976) and Modak (1979) on the effect of the H_2O and CO_2 absorption features in the spectra, shown in Table 2. It is also found in Fig. 2(a) or Fig. 2(b) that the peak value of 1100K curve is around 4.64 μm in wavelength scale (2156 cm^{-1} in wavenumber scale). This is obviously not consistent with the Wien's displacement law in its customary form $n\,\lambda_{max}T=2898$ μm-K. It is because that the experimental measurement output data are in the scale of wavenumber for Bomen software—GRAMS/32. From the fundamental Planck's distribution law, the spectral blackbody emissive power distribution for a black surface bounded by a transparent medium with refractive index n can be expressed can be expressed in both wavelength and wavenumber scale as (Bramson, 1968)

$$E_{b\lambda}(T,\lambda)=\frac{C_1}{n^2\lambda^5\left[e^{C_2/n\lambda T}-1\right]} \tag{1}$$

$$E_{b\eta}(T,\eta)=\frac{C_1\eta^3}{n^2\left[e^{C_2\eta/nT}-1\right]} \tag{2}$$

where $C_1=2\pi hc_0^2$, and $C_2=hc_0/k$. $k=1.3806\times10^{-23}$ J/K is Boltzmann's constant, $h=6.626\times10^{-34}$ Js is Planck's constant, and c_0 is the speed of light in vacuum. Eq. (2) may be transformed in wavelength scale with substituting η by $1/\lambda$ as

$$E^*_{b\lambda}(T,\lambda)=\frac{C_1}{n^2\lambda^5\left[e^{C_2/n\lambda T}-1\right]}. \tag{3}$$

The theoretical emission spectra of a blackbody at 1100K, 1200K and 1300K derived by Eq. (3) with $n=1$ are shown in Fig. 2(c). In comparison with Fig. 2(b), the experimental measurement data of the blackbody are generally consistent with the theoretical Planck's distribution law despite that the responses of Fig. 2(b) at the range of 14–20 μm have somewhat differences. The experiment data still show a small peak near 15 μm due to the absorption feature of CO_2.

To find the position of the maximum of Eq. (1) and Eq. (2), from the Wien's displacement law in both wavelength and wavenumber scale, they can be expressed as

$$n\,\lambda_{max}T=2898\ \mu\text{m-K}, \tag{4}$$

and

$$\eta_{max}/nT=1.961\ cm^{-1}/K. \tag{5}$$

As mentioned above, Eq. (9) is known as . Thus, if $n=1$, we can obtain from Eq. (10) that η_{max}=2157 cm^{-1} (4.63 μm), 2353 cm^{-1} (4.25 μm) and 2550 cm^{-1} (3.92 μm) at T=1100K, 1200K and 1300

K, respectively. Comparing the above theoretical data with the measured spectral peak value position in Fig. 2(b), it reveals that the experimental measurements are also in good agreement with the Wien's displacement law. Our experiments by the present instrument can be in good performance on measuring the emission spectrum of the emitting materials.

The system output (emissive power) data of our present measuring experiment are relative unit. In order to calculate the absolute unit of these responses, the instrument response function must be evaluated by comparing Fig. 2(b)—the recorded emission spectrum of our temperature-calibrated blackbody with Fig. 2(c)—the theoretical emission spectrum of a blackbody at the same temperature. Fig. 3 shows the instrument response function (IRF) of our present experimental measurement. The IRF is approximately a constant and reasonably good in the range 1.5–14 μm. As mentioned above, the data also have some small peaks at the absorption bands of H_2O and CO_2, and there are some unaccepted errors in the range of 14–20 μm.

Figs. 4(a) and 5(a) show the emission spectra of two quartz-tungsten-halogen lamps No. 64573 and No. 64743 at 30, 50 and 70 Volt, respectively, measured in the instrument enclosures with nitrogen gas purge. It is found that these emission spectra are superposed by three curves located in the ranges of about 1–4.5 μm, 4–9 μm and 9–20 μm, respectively. The emission spectrum probably consists with the emission from three different emitted materials. Increasing the voltage of the lamp increases the system output (emissive power) and shifts the peak value position to the short-wavelength regime. Figs. 4(b) and 5(b) show the emission spectra of the lamp immediately after it was switched off. The spectral curve with highest peak in either Fig. 4(a) or 5(a) disappears. While, there still exist the other two emission spectral curves located at about 4–9 μm and 9–20 μm. The emission spectrum from the lamp tungsten filament should be the responsibility for the curve with the highest peak in Fig. 4(a) or 5(a). One of two emission spectral curves in either Fig. 4(b) or Fig. 5(b) has some small peaks around 6 μm. According to the radiative properties of SiO_2, these bands were believed to be caused by the quartz envelope absorption. The spectral curve located at 4–9 μm should be corresponding to the emission from the warm quartz glass tube. The emission from the rest part of the whole lamp set (the base part) should be responsible for the other spectral curve located in the range 9–20 μm.

Fig 4(a) subtracted by Fig. 4(b), and Fig. 5(a) subtracted by Fig. 5(b) are, respectively, plotted in Fig. 4(c) and Fig. 5(c). They are the emission from the solely tungsten filament of the lamps at the different voltage of 30, 50 and 70 Volt. The measured data of the peak value position for No. 64573 lamp at different voltages are 2.4 μm (4160 cm^{-1}), 2.15 μm (4650 cm^{-1}) and 2.01 μm (4975 cm^{-1}), and those for No. 64743 lamp are 2.5 μm (4000 cm^{-1}), 2.33 μm (4290 cm^{-1}) and 2.17 μm (4610 cm^{-1}), respectively. At the different lamp voltage of 30, 50 and 70 Volt, the emission spectra ranging from 1–4.5 μm have the peak value position around 2.25 μm. Although the tungsten filament is not a perfectly blackbody, but in the short-wave region it is still a better emitter. They may be estimated by Eq. (5) that the corresponding tungsten filament temperatures range from 2000K to 2600K. The simultaneous measured filament temperatures by Infrared thermometer OS3709 for No. 64573 lamp are 2179K, 2486K and 2656K, and those for No. 64743 lamp are 2138K, 2363K and 2524K at 30, 50 and 70 Volt, respectively. Comparing these estimated temperatures with these measured temperatures, it reveals that they are principally in good agreement with the Planck's distribution law and Wien's displacement law. Increasing the lamp voltage will increase the lamp tungsten filament temperature and the system output (emissive power), and shift the highest peak value position to the short-wavelength regime. The spectral peak output of these heating sources range from 1.9–2.5 μm (4000–5200 cm^{-1}). Coupling with the instrument response function of Fig. 3, the total emissive power of the lamp in absolute unit can be calculated by integration from the finite wavelength band on the emission spectrum.

4. Conclusion

The emission spectrum measurement of the rapid thermal processing (RTP) heating source by Fourier Transform Infrared (FTIR) spectroscopy is presented. The work has been carried out on two quartz-tungsten-halogen lamps of OSRAM type No. 64573 and No. 64743 at the different lamp voltages of 30, 50, and 70 volt by Bomem MB-154 FTIR spectrometer ranging from 0.7 μm to 20 μm. From our present experimental measurement results, it is found that the emission spectrum is superposed by three spectral curves located in the range of about 1–4.5 μm, 4–9 μm and 9–20 μm, respectively, corresponding to the emission from the tungsten filament, the warm quartz glass tube and the base part. Increasing the lamp voltage will increase the lamp tungsten filament temperature and the system output (emissive power), and shift the highest peak value position to the short-wavelength regime. It also shows that the results are principally in good agreement with the Planck's distribution law and Wien's displacement law. The spectral peak output of these heating sources, corresponding tungsten filament temperatures from about 2000K to 2600K, range from 1.9–2.5 μm (4000–5200 cm^{-1}).

References

Bramson, M.A., *Infrared Radiation a Handbook for Applications*, Plenum Press, New York (1968).

Edward, D.K., "Molecular Gas Band Radiation," in *Advances in Heat Transfer*, Vol.12, Academic Press, New York, pp.115-193 (1976).

Griffiths, P.R., and Haseth, J.A., *Fourier Transform Infrared Spectrometry*, J. Wiley, New York (1986).

Modak, A.T., "Exponential Wide Band Parameters for the Pure Rotational Band of Water Vapor," *J. Quant. Spect. Radia. Trans.*, Vol.21, pp.131-142 (1979).

Noel, S., Ventura, L., Slaoui, A., Muller, J.C., Groh, B., Schindler, R., Froschle, B., and Theiler, T., "Impact of Ultraviolet Light during Rapid Thermal Diffusion," *Appl. Phys. Lett.*, Vol.72, No.20, pp.2583-2585 (1998).

Ravindra, N.M., Abedrabbo, S., Chen, W., Tong, F.M., Nanda, A.K., and Speranza, A.C., "Temperature-Dependent Emissivity of Silicon-Related Materials and Structures," *IEEE Trans. Semiconduct. Manufact.*, Vol.11, No.1, pp.30-39 (1998).

Roozeboom, F., and Parekh, N., "Rapid Thermal Processing Systems: A Review with Emphasis on Temperature Control," *J. Vac. Sci. Technol.*, Vol.B8, No.6, pp.1249-1259 (1990).

Sikka, K.K., "High Temperature Normal Spectral Emittance of Silicon Carbide Based Materials," M.S. thesis, The Pennsylvania State University, University Park (1991).

Singh, R., "Rapid Isothermal Processing", *J. Appl. Phys.*, Vol.63, No.8, pp.R59-R114 (1988).

Singh, R., Sinha, S., Thakur, R.P.S., and Chou, P., "Some Photoeffect Roles in Rapid Isothermal Processing," *Appl. Phys. Lett.*, Vol.58, No.11, pp.1217-1219 (1991).

Sorrel, F.L., Yu, S., and Kiether, W.J., "Applied RTP Optical Modeling: An Argument for Model-Based Control," *IEEE Trans. Semiconduct. Manufact.*, Vol.7, pp.454-459 (1994).

Timans, P.J., "The Role of Thermal Radiative Properties of Semiconductor Wafers in Rapid Thermal Processing," *Mat. Res. Soc. Symp. Proc.*, Vol.429, pp.3-14 (1996).

Wong, P.Y., Miaoulis, I.N., and Madras, C.G., "Transient and Spatial Radiative Properties of Patterned Wafers during Rapid Thermal Processing," *Mat. Res. Soc. Symp. Proc.*, Vol.387, pp.15-27 (1995).

Zhou, Z.H., and Reif, R., "Epi-Thickness Measurements Using Emission Fourier Transform Infrared Spectroscopy-Part I: Sensor Characterization," *IEEE Trans. Semiconduct. Manufact.*, Vol.8, No.3, pp.333-339 (1995).

Table 1 MIKRON M330 Blackbody temperature checked by Infrared thermometer OS3709 and K-type thermocouple

M330 Blackbody setting temperature (℃)	900	950	1000	1050	1100	Mean Error
Temperature (℃) measured by Infrared Thermometer	904.5	950.4	997	1046	1092	
Error (%)	+0.5	+0.04	-0.3	-0.38	-0.78	0.39
Temperature (℃) measured by Thermocouple K-type	894	943	994	1045	1093	
Error (%)	-0.67	-0.74	-0.6	-0.48	-0.64	0.63

Table 2 H_2O and CO_2 spectral absorption features (Edwards, 1976; Modal, 1979)

H_2O	1.38 μm	1.87 μm	2.7 μm	6.3 μm		
CO_2	2.0 μm	2.7 μm	4.3 μm	9.4 μm	10.4 μm	15 μm

Fig. 1: Schematic diagram of FT-IR apparatus.

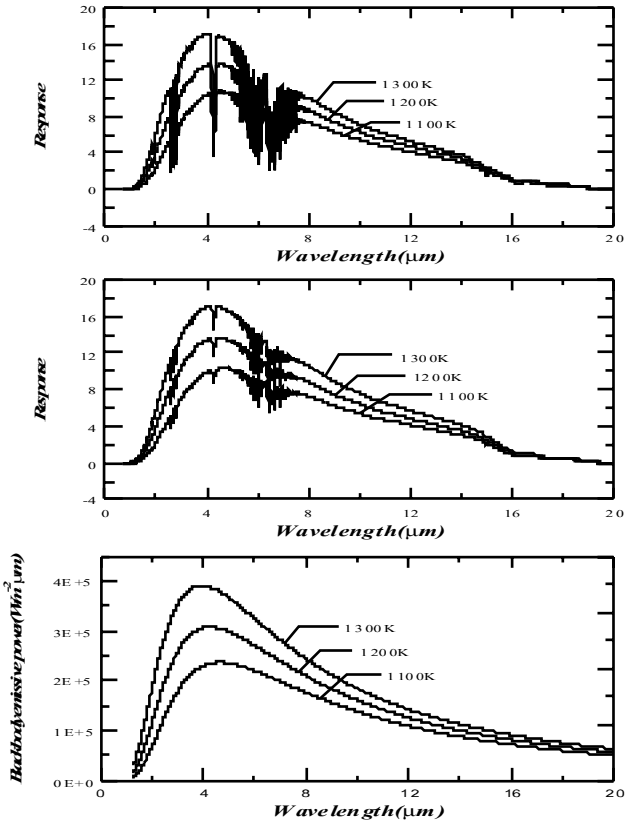

Fig. 2: Emission spectra: (a) temperature-calibrated blackbody without nitrogen gas purge; (b) temperature-calibrated blackbody with nitrogen gas purge; (c) theoretical calculation blackbody curve by Eq. (5) for Planck's distribution law.

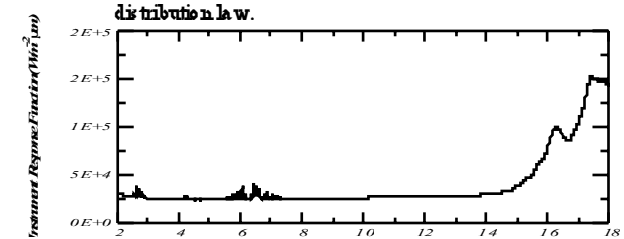

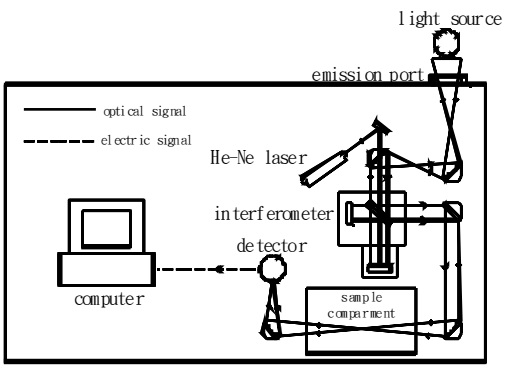

Fig. 3: Response function of the instrument.

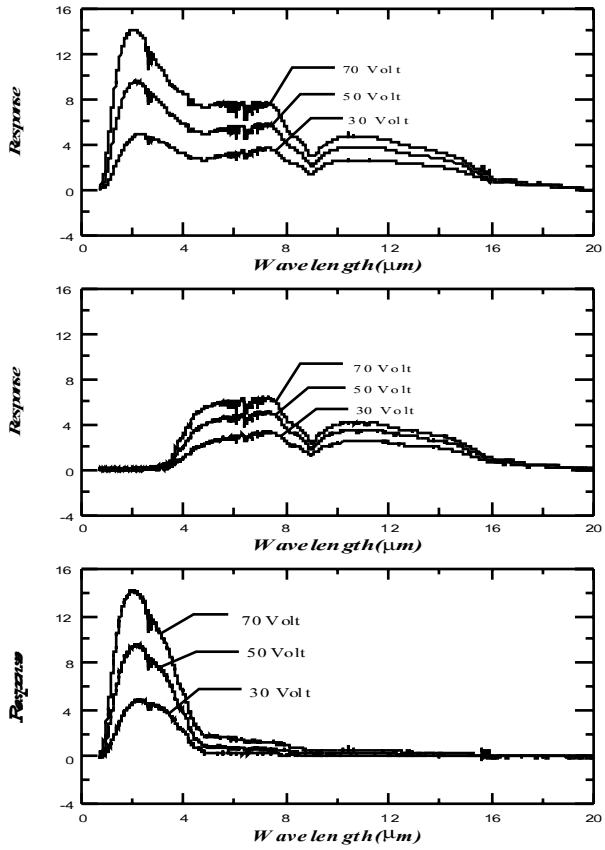

Fig. 4: Emission spectra of ORSAM No. 64573 quartz-tungsten-halogen lamp: (a) whole lamp set (b) after switching off lamp; (c) the tungsten filament.

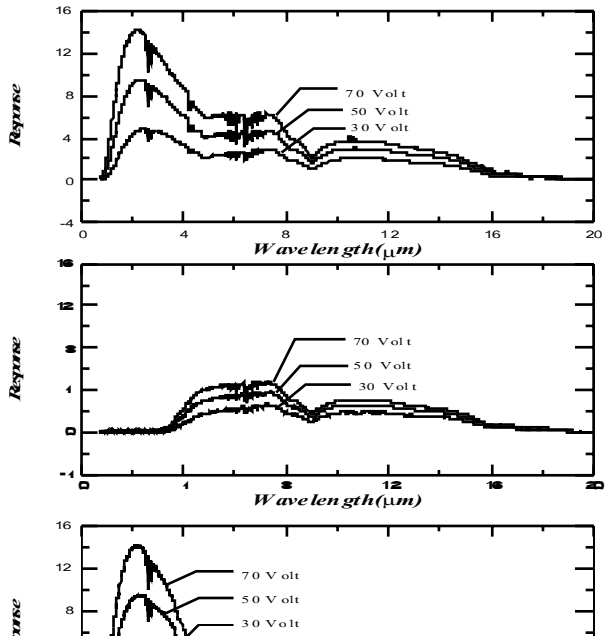

Fig. 5: Emission spectra of ORSAM No. 64743 quartz-tungsten-halogen lamp: (a) whole lamp set, (b) after switching off lamp, (c) the tungsten filament.